Influence of the surface on the transverse magnetoresistance of bismuth

S. S. Murzin

Institute of Solid State Physics, USSR Academy of Sciences
(Submitted 10 August 1981)
Zh. Eksp. Teor. Fiz. **82**, 515–527 (February 1982)

The transverse magnetoresistance of a bismuth plate in which almost the entire current flow is concentrated at the surface is investigated experimentally. The magnetoresistance is found to depend strongly on the angle between the magnetic field and the plane of the plate, decreases with decreasing temperature when the temperature is lowered, and has a nonmonotonic dependence on the temperature in an oblique magnetic field. Deviations from Ohm's law are observed at large currents through the sample. The resistance of a semimetal plate in a magnetic field inclined to the plane of the plate is determined phenomenologically with account taken of the effect of the surface. In relatively strong magnetic fields the experimental results agree well with the theory and can be used to determine a number of properties of the samples. In weaker fields, however, appreciable qualitative deviations of the experimental data from the theory are observed.

PACS numbers: 73.25. + i

In a strong magnetic field, where the average electron-orbit radius is much less than the mean free path, $r \ll l$, the surface can affect the galvanomagnetic properties of a compensated metal strongly for two reasons. First, the electron mobility is much higher in a surface layer of thickness $\sim r$ than in the interior, since the centers of the electron orbits are more frequently shifted by collisions with the surface.[1] Second, in crossed electric and magnetic fields the drift of the carriers changes their density at the surface. The density gradients cause diffusion of the electrons and of the holes. The high carrier mobility and the diffusion fluxes near the surface make the conductivity of the surface layer much higher than that of the interior of the metal. The distribution of the direct current over the sample thickness becomes nonuniform—the current is concentrated near the metal surface.

The effect of the surface on the magnetoresistance of metals was considered by a number of workers.[1-6] The case when the probabilities of the intervalley and intravalley scattering in the interior coincide and the diffusion processes have no effect was investigated in Refs. 1–4. The surface current is then concentrated in a surface layer having a thickness of the order of r.

In semimetals, the time of intervalley relaxation T_{int} is much longer than the intravalley relaxation time τ. In this case, which is dealt with in Refs. 5 and 6, diffusion processes assume a major role. Surface scattering influences the conductivity up to the distances, of the order of diffusion length L, over which the density gradients fall off and the current density becomes equal to its bulk value. In a magnetic field parallel to the surface, $L = L_0 \sim r(T_{int}/\tau)^{1/2}$.

The effect of the surface on the galvanomagnetic properties of bismuth was the subject of a number of studies,[5,7,8] in which the dependences of the resistivity on the magnetic field and on the sample thickness were investigated in a field parallel to the surface. Shape effects were observed also in Refs. 7 and 8. The results of Hattori[5] are in satisfactory agreement with the theoretical deductions in magnetic fields up to 1 kOe. Noticeable deviations are observed in stronger fields and are attributed by Hattori to the dependence of the carrier surface recombination rate on the magnetic fields. The results of Bogod *et al.*,[7,8] obtained in magnetic fields 1–16 kOe, do not agree with the theory.

Additional information on the surface conductivity σ_{sur} of bismuth can be obtained by investigating the dependences of the conductivity on the temperature and on the angle α between the magnetic field and the sample surface. According to the theory of Refs. 5 and 6, σ_{sur} should increase with decreasing temperature, whereas the bulk conductivity σ_b decreases in a transverse magnetic field.

The angular dependence of σ_{sur} is due to the increase of the diffusion length with increasing angle between the magnetic field and the surface,

$$L \sim [r^2 + (l\alpha)^2]^{1/2} (T_{int}/\tau)^{1/2}$$

(see below). Even at $\alpha \ll 1$, the length L can greatly exceed the diffusion length L_0 in a magnetic field parallel to the surface if $\alpha \gg r/l$ $(r/l \ll 1)$.

We have investigated experimentally the transverse magnetoresistance of bismuth plates in which almost the entire current flowing through the plates was concentrated at the surface. The magnetoresistance was investigated as a function of the magnetic field, of the angle α between the magnetic field and the surface, and the temperature: $\rho_\phi = \rho_\phi(H, \alpha, T)$. In addition, manifestations of the nonlinear properties were observed on the current-voltage characteristics. The problem of the conductivity of a semimetal plate in a magnetic field inclined to the surface was solved phenomenologically (only a magnetic field parallel to the surface was considered in Refs. 5 and 6).

CONDUCTIVITY OF A SEMIMETAL PLATE IN A MAGNETIC FIELD INCLINED TO THE SURFACE

We shall solve the problem phonomenologically, in the manner used to solve the analogous problem for a magnetic field parallel to the surface[5] and the problem

 0038-5646/82/020298-08$04.00

of anisotropic size effects without a magnetic field.[9] We present first the solution for the simple case of a compensated semimetal with one electron valley and one hole valley, and then discuss the changes that must be introduced into the solution to take the real Fermi surface of bismuth into account.

Let the Fermi surface of the semimetal have in each of the valleys the form of an ellipsoid with one of its principal axes normal to the plate surface (the y axis), and the other parallel to the electric current (the x axis). The magnetic field vector $\mathbf{H}$ lies in the yz plane and makes a small angle $\alpha \ll 1$ with the z axis. The electron and hole valleys are far from each other in momentum space, so that the following condition is satisfied at low temperatures:

$$\tau/T_{\text{int}} \ll 1.$$

Since the intravalley relaxation of the carriers is much faster than the intervalley relaxation, a separate conductivity tensor can be introduced for each valley. In our case, the electron and hole conductivity tensors in a strong magnetic field $r \ll l$ are given by

$$\hat{\sigma}_{e,h} = \begin{pmatrix} \sigma_1^{e,h} & \sigma_H^{e,h} & \alpha\sigma_H^{e,h} \\ -\sigma_H^{e,h} & \sigma_2^{e,h}+\alpha^2\sigma_3^{e,h} & -\alpha\sigma_3^{e,h} \\ -\alpha\sigma_H^{e,h} & -\alpha\sigma_3^{e,h} & \sigma_3^{e,h} \end{pmatrix}, \tag{1}$$

$$\sigma_1^{e,h},\ \sigma_2^{e,h} \sim \sigma_3^{e,h}\left(\frac{r}{l}\right)^2, \quad \sigma_H{}^{e} = -\sigma_H{}^{h} = \frac{nec}{H} \equiv \sigma_H \sim \sigma_3^{e,h}\frac{r}{l}.$$

The indices e and h label respectively the electrons and holes, $\sigma_3^{e,h}$ is independent of the magnetic field, n is the electron or hole density ($n_e = n_h = n$), e is the electron charge, and c is the speed of light. The electric current is connected with the electric field and with the density gradients:

$$\mathbf{j} = \mathbf{j}_e + \mathbf{j}_h = (\hat{\sigma}_e + \hat{\sigma}_h)\mathbf{E} + e\hat{D}_e\nabla n - e\hat{D}_h\nabla n. \tag{2}$$

By virtue of the electroneutrality we have $\nabla n_e = \nabla n_h \equiv \nabla n$. The conductivity and diffusion tensors of each of the valleys are connected by the Einstein relation

$$e\hat{D}_{e,h} = \hat{\beta}_{e,h}\hat{\sigma}_{e,h}, \quad \beta_{e,h} = 1/e\nu_{e,h},$$

$\nu_{e,h}$ are the state densities of the electrons and holes on the Fermi level. The current flows in the plate along the x axis. From (2) we obtain

$$j_x = (\sigma_1{}^{e} + \sigma_1{}^{h})E_x + \sigma_H(\beta_e + \beta_h)\nabla n. \tag{3}$$

The influence of the surface is due to the presence of the second term in (3). To determine the plate resistivity we must find ∇n as a function of y and of E_x. Using the condition $j_y^e + j_y^h = 0$, the continuity equation in the following form at small deviations n' of the carrier density from its equilibrium value n_0 ($n' = n - n_0$, $n' \ll n_0$)

$$\partial j_y{}^{e}/\partial y = n'e/T_{\text{int}}$$

and the equality (2), we obtain

$$\frac{\partial}{\partial y}[-\sigma_H E_x + (\beta_e + \beta_h)\sigma\nabla n'] = \frac{n'}{T_{\text{int}}}e; \tag{4}$$

here

$$\sigma = \frac{(\sigma_2{}^{e}+\alpha^2\sigma_3{}^{e})(\sigma_2{}^{h}+\alpha^2\sigma_3{}^{h})}{\sigma_2{}^{e}+\alpha^2\sigma_3{}^{e}+\sigma_2{}^{h}+\alpha^2\sigma_3{}^{h}}.$$

Linearizing the left-hand side of (4), we get

$$(\beta_e+\beta_h)\sigma\frac{\partial^2 n'}{\partial y^2} = \frac{n'}{T_{\text{int}}}e. \tag{5}$$

The solution of this equation is $n' = n_1\exp(-y/L) + n_2 \times \exp(y/L)$, where

$$L = [(\beta_e+\beta_h)\sigma T_{\text{int}}/e]^{1/2}. \tag{6}$$

The constants n_1 and n_2 are obtained from the boundary conditions on the plate faces, which lie in the planes $y = 0$ and $y = d$. These boundary conditions are of the form

$$j_y{}^{e} = -\sigma_H E_x + (\beta_e+\beta_h)\sigma\frac{\partial n'}{\partial y}\Big|_{y=0,d} = \pm Sn'e, \tag{7}$$

S is the rate of the carrier surface recombination and is given by

$$S = {}^1\!/_4 v_{Fy}{}^{e}\tilde{d}_{e-h} + {}^1\!/_4 v_{Fy}{}^{h}\tilde{d}_{h-e}.$$

Here $v_{Fy}^{e,h}$ are the velocities of the electron and holes having the Fermi energy and moving parallel to the y axis; $\tilde{d}_{e-h}$ and $\tilde{d}_{h-e}$ are the fractions of the intervalley surface scattering of the electrons and holes. If N_e electrons are incident in a time Δt on the surface, and N_e' electrons go over into the hole valley after colliding with the surface, then $\tilde{d}_{e-h} = N_e'/N_e$. From the condition that the electrons and holes be in equilibrium if no current flows through the sample, it follows that

$$v_{Fy}{}^{e}\tilde{d}_{e-h}\nu_e = v_{Fy}{}^{h}\tilde{d}_{h-e}\nu_h. \tag{8}$$

Substituting the solution of Eq. (5) with boundary conditions (7) in Eq. (3) and integrating the current density over the entire plate thickness from 0 to d, we obtain the connection between the total current through the sample and the electric field E_x. The current in a sample of thickness $d \gg L$ is

$$I = \left[(\sigma_1{}^{e}+\sigma_1{}^{h})d + 2(\beta_e+\beta_h)\frac{\sigma_H{}^{2}e^{-1}}{S+L/T_{\text{int}}}\right]E_x. \tag{9}$$

This result agrees with a microscopic calculation[6] for a magnetic field parallel to the surface at $\tilde{d}_{e-h}$, $\tilde{d}_{h-e} \ll 1$.

We consider now the case when the surface conductivity [the second term of (9)] is much larger than the bulk conductivity $(\sigma_1^e + \sigma_1^h)d$. A plate of unity length and unity width has then a resistivity

$$\rho_p = \frac{S + L/T_{\text{int}}}{2(\beta_e+\beta_h)\sigma_H{}^{2}}e. \tag{10}$$

Figure 1 shows a plot of ρ_p vs. α as given by Eq. (10).

At $(r/l)^2 \ll \alpha^2 \ll 1$ the ratio L/T_{int} is of the order of $|\alpha|v_F(\tau/T_{\text{int}})^{1/2}$. The resistivity can be represented in the form $\rho_p = \rho_0 + |\alpha|\rho_1$, where

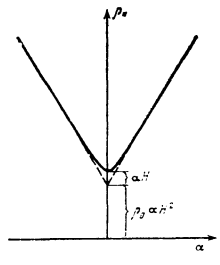

FIG. 1.

$$\rho_0=\frac{Se}{2(\beta_e+\beta_h)\sigma_{H^2}}\propto H^2,\quad \rho_1=\frac{1}{2\sigma_{H^2}}\left[\frac{\sigma_3^e\sigma_3^h}{\sigma_3^e+\sigma_3^h}\frac{e}{\beta_e+\beta_h}\frac{1}{T_{\text{int}}}\right]^{1/2}\propto H^2\left(\frac{\tau}{T_{\text{int}}}\right)^{1/2}. \tag{11}$$

At $\alpha^2\ll(r/l)^2$ the resistivity is the sum of a term ρ_0 proportional to H^2, and a term proportional to H (see Fig. 1, since

$$L/T_{\text{int}}\sim r/(\tau T_{\text{int}})^{1/2}\propto 1/H.$$

We proceed now to a discussion of the results for more complicated Fermi surfaces. If the principal axes of the ellipsoids are not parallel to the axes x, y, z or if the Fermi surfaces of each of the valleys are not ellipsoids, but there is only one electron and one hole valley as before, the conductivity tensors are more complicated than the tensor (1). Equations (6), (10), and (11) are valid in this case, although the connection between the surface recombination rate S and $\tilde{d}_{e-h}$ or $\tilde{d}_{h-e}$ and the electron-hole equilibrium condition (7) are different.

The Fermi surface of bismuth consists of three electron ellipsoids and one hole ellipsoid. To solve the problem in this case it is necessary to introduce for each of the electron and hole valleys a separate conductivity tensor, a continuity equation, and boundary conditions similar to (7). Solutions of the problem in a number of cases corresponding to experimental conditions are given in the Appendix.

The answers are more complicated than for the two-valley model. In particular, the angular dependences are more complicated at $(r/l)^2\ll\alpha^2\ll 1$. In limiting cases (see the Appendix) the functions $\rho_\phi(\alpha)$ reduce to the form $\rho_\phi=\rho_0+\rho_1|\alpha|$. Then $\rho_0\propto H^2$ and $\rho_1\propto H^2$, i.e., the results agree qualitatively with the results for the two-valley model.

SAMPLES AND PROCEDURE

The experiments were performed on single-crystal bismuth plates. Rectangular plates and disks were used (see Fig. 2). The geometric dimensions of the samples and the orientation of the crystallographic axes C_1, C_2, and C_3 are indicated in Table I. Samples 1–3 were cut from a single-crystal ingot grown by the Czochralski method with a filament moistened by nitric acid. The ratio of the ingot room and helium temperatures was 840. The remaining samples were grown in a polished quartz mold.

The surfaces of samples 1–3 were finished by two methods:

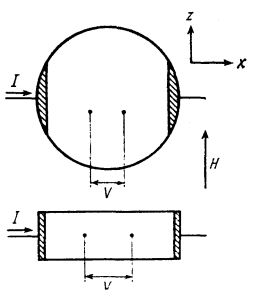

FIG. 2. Wiring of samples.

TABLE I.

Bi samples	Crystallographic axis normal to plate surface	Current along crystallographic axis	Plate thickness d, mm	Plate width h, mm*	ρ_ϕ at $T=4.2°$ 10^{-3} Ω/kOe	$\frac{\rho_\phi}{10^{-3}}$ Ω/kOe²	$s\cdot10^4$ cm/sec	$\tilde{d}_{e-h}\cdot10^3$	$\tilde{d}_{h-e}\cdot10^3$
1	C_3	C_2	0.5	2.8	2.1	4.0	4.9	1.0	16
2	C_3	C_2	1.45	2.8	–	–	–	–	–
3	C_3	C_2	2.4	2.8	–	–	–	–	–
4	C_3	C_2	1	6	1.2	8.5	10.4	2.1	33
5	C_3	C_2	0.8	17.8	0.9	4.3	5.3	1.1	17
6	C_3	C_2	1.2	6	1.3	2.0	2.4	0.5	7.7
7	C_3	C_2	0.4	17.8	1.4	0.4	0.5	0.1	1.6
8	C_1	C_2	1	10	2.6	16.5	>20	>5.2	>20
9	C_2	C_1	1	10	1.8	13.0	>16	>3.7	>16

*Samples 5, 7, 8, and 9 were disks. The number in the column is the diameter.

1) Etching with 35% nitric acid, washing with distilled water, and storing 16 hours in distilled water, and storing 16 hours in distilled water. The surface was coated as a result by a thin oxide film and was brownish in color.

2) Etching with a 25% HNO_3 + 35% H_3PO_4 + 35% H_2O solution.

The surface of sample No. 4 was finished by the first method. The surfaces of the remaining samples were formed during the crystal growth in the mold.

The resistance was measured by the four-point method. The current-carrying leads were secured with a conducting adhesive (shaded regions in Fig. 2). The potential leads were clamped to the sample surfaces. The use of disks to measure the transverse magnetoresistance is not accompanied by noticeable errors due to the inhomogeneous distribution of the current along the x and z axes, provided that the distance between the potential contacts, which are located at the center of the sample, is much shorter than the disk diameter, and the magnetic field is parallel or inclined at a small angle α to the disk surface. The reason is that in a strong magnetic field ($r\ll l$) the longitudinal conductivity of a compensated metal is much larger than the transverse one. The equipotential surfaces in the sample are therefore parallel to the magnetic field. The distribution of the current density j and of the electric field

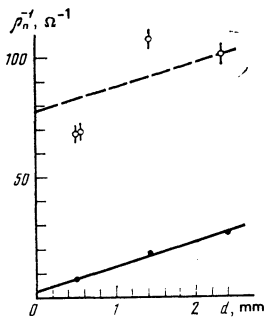

FIG. 3. Reciprocal resistivity ρ_ϕ^{-1} of the plates vs. the thickness d for various surface finishes. Samples 1, 2, and 3 differ in thickness. Each was treated by two methods: o) surface etched with HNO_3 and oxidized; •) surfaces etched with mixture of HNO_3 and H_3PO_4; $H=1$ kOe, $\alpha=0$.

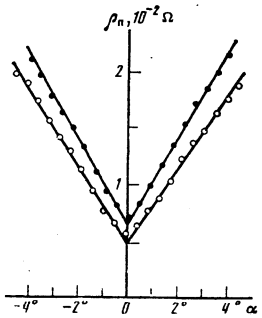

FIG. 4. Dependence of resistivity ρ_ϕ on the angle between the magnetic field and the plate surface for sample Bi6: ●) $T = 4.2$ K, ○) $T = 1.6$ K; $H = 1.46$ kOe.

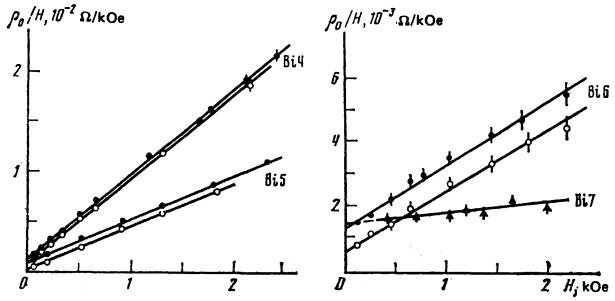

FIG. 5. Dependence of ρ_0/H on the magnetic field H: ●, ▲) $T = 4.2$ K, ○) $T = 1.6$ K.

along the axes x and z is almost uniform between two close equipotential surfaces that pass through the potential contacts.

The samples were placed directly in liquid helium. The magnetic field was produced by a superconducting solenoid. The measurements were made in magnetic fields weaker than 3 kOe to exclude quantum effects that affect strongly the magnetoresistance in stronger field if $\mathbf{H} \parallel C_1$ or $\mathbf{H} \parallel C_2$.

As seen from Fig. 3, the magnetoresistance depends strongly on the method used to finish the surface. In our experiments, the sample thickness d exceeded the diffusion length L, so that the reciprocal of the resistivity ρ_ϕ^{-1} (ρ_ϕ is the resistivity referred to a unit length and width of the sample) can be divided into two terms, $\rho_\phi^{-1} \equiv \sigma_b d + \sigma_{sur}$. The slope of the lines in Fig. 3 yields the value of the bulk conductivity σ_b, and the intercept with the ordinate axis the surface conductivity σ_{sur}. The surface conductivity σ_{sur} of the samples treated with HNO_3 and oxidized is much higher than the bulk conductivity σ_b.

The experimental results that follow were obtained with plates having σ_{sur} much larger than $\sigma_b d$. In the better samples, $\sigma_{sur}/\sigma_b d \sim 100$.

EXPERIMENTAL RESULTS

The results were qualitatively the same for all samples with $\sigma_{sur} \gg \sigma_b d$, regardless of the surface treatment and of the crystallographic orientation.

In a magnetic field H of constant magnitude the magnetoresistance increases when the magnetic field is tilted away from the plane of the plate through a small angle α. The angular dependence for the sample Bi6, shown in Fig. 2, can be represented in the form $\rho_\phi(\alpha) = \rho_0 + |\alpha|\rho_1$. For many samples, this formula describes the results only at $\alpha \gtrsim 1°$. At lower α, the angular dependence becomes slower, and the resistivity $\rho_\phi(0)$ in a magnetic field parallel to the surface exceeds the value ρ_0 that can be determined by extrapolating the linear sections of the angular dependence to $\alpha = 0$. This behavior of $\rho_\phi(\alpha)$ agrees qualitatively with the calculation result (see Fig. 1). There is, however, another reason why $r_\phi(0)$ exceeds ρ_0, namely the surface roughness of the plate. Different sections of the rough surface are inclined to one another, so that even if the surface is on the average parallel to the magnetic field ($\alpha = 0$), its individual sections are not parallel to the field. This increases the resistivity $\rho_\phi(0)$. To exclude the effect exerted on the surface by the surface relief, we investigated the values of ρ_0 and ρ_1, which describe the resistivity in the region linear in α.

Figure 5 shows plots of ρ_0/H against H for samples with different surfaces. The experimental points are well fitted by straight lines, so that ρ_0 for each sample can be represented in the form $\rho_0 = \rho_2 H + \rho_3 H^2$. The value of ρ_2 is determined by the incercept of the line $\rho_0/H = \rho_2 + \rho_3 H$ with the ordinate axis, and ρ_3 from the slope of the line. The lines corresponding to one sample at different temperatures are parallel (see Fig. 5), and the line for $T = 1.6$ K lies lower than the line for $T = 2.4$ K. This means that ρ_3 is independent of temperature, and that ρ_2 is smaller at 1.6 K than at 4.2 K. To obtain more detailed information on the temperature dependence of ρ_2, measured the temperature dependences of ρ_ϕ in a magnetic field parallel to the surface of the plate. These dependences are shown in Fig. 6 for the samples Bi5 and Bi6. These samples had even surfaces, and in a magnetic field parallel to the surface they had $\rho_\phi \approx \rho_0$. The dependence of ρ_2 on T in a fixed magnetic field H_0 can be obtained by subtracting from $\rho_\phi \approx \rho_0$ the quantity $\rho_3 H_0^2$, which does not depend on temperature. In Fig. 6 the quantities $\rho_3 H_0^2$ are shown by dashed lines. In a strong magnetic field, where the linear term $\rho_2 H$ is small compared with the quadratic $\rho_3 H^2$ ($H \gg \rho_2/\rho_3$), and therefore $\rho_\phi \approx \rho_0 \approx \rho_3 H^2$ at $\alpha = 0$, and ρ_ϕ is practically independent of temperature. This con-

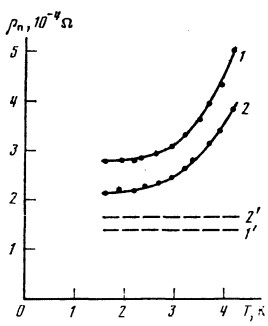

FIG. 6. Temperature dependence of the resistivity ρ_ϕ in a magnetic field parallel to the surface. Curve 1) sample Bi6, $H = 260$ Oe, curve 2) Bi4, $H = 195$ Oe.

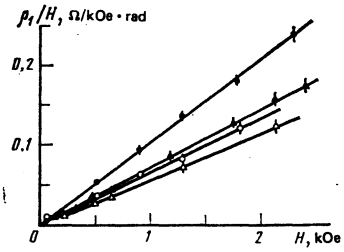

FIG. 7. Dependence of ρ_1/H on the magnetic field H. Sample Bi4: ●) $T = 4.2$ K, ○) $T = 1.6$ K. Sample Bi5: ▲) $T = 4.2$ K, △) $T = 1.6$ K.

firms the conclusion that ρ_3 does not depend on T in the temperature interval 1.6–4.2 K.

The values of ρ_2 and ρ_3 obtained from a reduction of the field dependences are listed in Table I. The values of ρ_2 are close at $T = 4.2$ K for samples Bi4–Bi7, which have the same orientation, whereas the ρ_3 of different samples differ strongly.

The dependence of the resistivity $\rho_{\hbar}$ on α is determined by the value of ρ_1. Figures 7 and 8 show plots of ρ_1/H vs. the magnetic field H for samples with different surfaces. The lines passing through the origin correspond to quadratic dependences of ρ_1 on H. It is seen from the figures that the experimental ρ_1 are nearly quadratic in H, although deviations in weak fields are observed in some samples, e.g., Bi6 and Bi7 (see Fig. 8). It can be noted that these deviations take place only in magnetic fields $H < \rho_2/\rho_3$. In samples Bi6 and Bi7, whose ρ_2/ρ_3 are larger than those of others, the deviations from the relation $\rho_1 \propto H^2$ start in stronger fields. In sample Bi4, whose ρ_2/ρ_3 is small, a noticeable deviation from the straight line corresponding to $\rho_1 \propto H^2$ is observed only for one extreme-left point (light circle in Fig. 7) in a field 65 Oe. It is seen from Figs. 7 and 8 that wherever ρ_1 ceases to be quadratic in H a change takes place in the $\rho_1(T)$ temperature dependence.

The dependence of ρ_1 on T was investigated in detail in the field range in which $\rho_1 \propto H^2$. It turned out that in this case ρ_1 varies nonmonotonically with decreasing temperature in all samples. Examples of nonmonotonic dependences of ρ_1 on T are shown in Fig. 9.

DISCUSSION

In a strong magnetic field $H \gg \rho_2/\rho_3$, where the linear terms in ρ_0 can be neglected, the experimental results

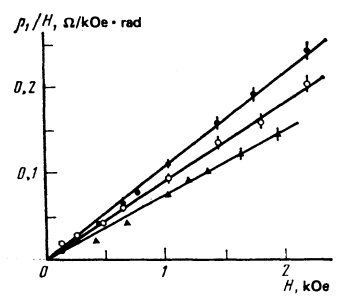

FIG. 8. Dependence of ρ_1/H on the magnetic field H. Sample Bi6: ●) $T = 4.2$ K, ○) $T = 1.6$ K. Sample Bi7: ▲) $T = 4.2$ K.

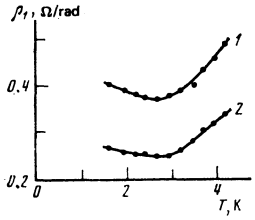

FIG. 9. Dependence of ρ_1 on the temperature T: curve 1) sample Bi6, $H = 2.21$ kOe. 2) Bi4, $H = 2.15$ kOe.

agree well with the calculation. Namely, there are regions where $\rho_{\hbar}$ is linear in α, ρ_0 and $\rho_1 \propto H^2$, and ρ_0 does not depend on temperature. The nonmonotonic temperature dependence of ρ_1 is due to the nonmonotonic temperature dependences of the time ratio $\tau/T_{int}[\rho_1 \propto (\tau/T_{int})^{1/2}$, see Eq. (11)].

Indeed, in bismuth at helium temperatures the frequency of intervalley transitions of carriers scattered by phonons decreases exponentially with decreasing temperature,[10] and the frequency of the intravalley scattering by phonons decreases more slowly, in accord with a power law. Therefore, so long as the frequency of the intervalley transitions resulting from the electron-phonon interaction exceeds the frequency of the intervalley transitions in scattering by impurities and crystal-lattice defects, the ratio τ/T_{int} will decrease with decreasing temperature. Since, however, T_{int} changes more rapidly than τ, it reaches more rapidly the temperature-independent level determined by the scattering of the electrons and holes by the impurities and defects. With further decrease in temperature, the behavior of the ratio τ/T_{int} is determined by the temperature dependence of the time τ, which increases with decreasing temperature. Thus, τ/T_{int} has a nonmonotonic temperature dependence.

In the field region $H \gg \rho_2/\rho_3$ the experimental results can be reduced with the aid of Eqs. (10)–(12). It was assumed in the calculations that the hole spectrum is quadratic, the electron spectra are not quadratic, but the Fermi surfaces in each of the valleys are ellipsoids. The following parameters of the bismuth energy spectrum were used: electron and hole density $n_0 = 3 \times 10^{17}$ cm^{-3}, hole Fermi energy $\mathscr{E}_F^h = 11.7$ meV, the hole velocity in the directions C_1 and C_2 is $v_1^h = v_2^h = 2.5 \times 10^7$ cm/sec, the hole velocity in the C_3 direction is $v_3^h = 0.77 \times 10^7$ cm/sec, and the electron velocity along C_3 is $v_3^e = 7.5 \times 10^7$ cm/sec. The state density on the Fermi level in the hole valley is $\nu_h = 3n_0/2\mathscr{E}_F^h$. The electron state density was obtained by subtracting the hole state density ν_h from the total state density $\nu_e + \nu_h = 6.2 \times 10^{31}$ erg^{-1}·cm^{-3}, determined by measuring the electronic heat capacity of bismuth.[11] The experimental value of the heat capacity obtained in Ref. 11 agrees with the calculation of Ref. 12.

The surface recombination rates calculated from the measurements are listed in Table I. For the Bi7 sample, $H < \rho^2/\rho^3$ in the entire magnetic-field range in which the measurements were made. In this range, which will be discussed below, theory does not agree with experiment. Since, however, the formula $\rho_0 = \rho_2 H$

$+\rho_3 H^2$ describes the results for other samples both at $H \ll \rho_2/\rho_3$ and at $H \gg \rho_2/\rho_3$, and in a strong field ($H \gg \rho_2/\rho_3$) we have $\rho_0 = \rho_3 H^2$, we likewise determined S for Bi7 by assuming that

$$\rho_3 H^2 = Se/2(\beta_e + \beta_h)\sigma_H^2.$$

The surface-recombination rate was used to determine the values of $\tilde{d}_{e-h}$ and $\tilde{d}_{h-e}$. They are listed in Table I.

The samples Bi8 and Bi9 were measured with the crystallographic C_3 axis directed along z. In this case (see the Appendix) Eq. (11) holds for ρ_1. Recognizing that $\sigma_3^h \ll \sigma_3^e$ and $\sigma_3^h = ne^2\tau_h/m_{33}$ (m_{33} is the effective mass of the holes along the C_3 axis), and knowing ρ_1, we can determine T_{int}/τ_h. For Bi8 at $T = 4.2$ K we have $T_{int}/\tau_h = 70$, and for Bi9 we have $T_{int}/\tau_h = 110$ and 50 at $T = 1.6$ and 4.2 K, respectively.

In magnetic fields $mc/e\tau \ll H \lesssim \rho_2/\rho_3$ the experimental results differ markedly from the calculated ones. First, the experimental $\rho_0(H)$ dependence is of the form $\rho_0 = \rho_2 H + \rho_3 H^2$, whereas the theory predicts a dependence in the form $\rho_0 \propto H_2$. [We note that in Ref. 5, in which the measurements were made only at $\alpha = 0$, the resistivity term linear in H was associated with the linear term shown in Fig. 1. The procedure we used to reduce the experimental data yielded the value of $\rho_0(H)$ directly and avoided the uncertainties in the interpretation of the derived relations.] Secondly, the theory calls for $\rho_1 \propto H^2$, whereas the experimental points deviate from this dependence in the magnetic-field region in question.

The discrepancy between the experiment and the calculation in fields $mc/e\tau \ll H \lesssim \rho_2/\rho_3$ is possibly due to the fact that the phenomenological approach is not justified under these conditions. A shortcoming of the phenomenological solution is that the conductivity tensors introduced for the bulk metal are not valid at distances of the order of r from the surface. Babkin and Kravchenko[6] solved the problem using a microscopic approach for the cases of specular and diffuse intravalley scattering in a magnetic field parallel to the surface. Their results at $\tilde{d}_{e-h} \ll 1$ agree with ours for $\alpha = 0$. It is possible that a microscopic solution of the problem in a magnetic field inclined to the surface or in the case when the scattering from the surface is more complicated in character than just specular or diffuse will lead to a result that agrees better with experiment than those of the phenomenological approach.

The region in which the phenomenological solution describes the experimental results, and the region in which experiment and theory do not agree, have as their boundary the magnetic field $H_c = \rho_2/\rho_3$. We note that in all our samples the distance $r_c/\tilde{d}_{e-h}$ negotiated by the electrons that hop over the surface in a magnetic field H_c (r_c is the Larmor radius of the electrons in the field H_c) are of the order of 1 mm. The mean free path $l \sim r_c/\tilde{d}_{e-h}$ is of the same order.

NONLINEAR PROPERTIES

The described results are valid for weak electric fields and currents, when Ohm's law holds. At larger current flow through the sample, the resistance is higher than in the ohmic region, and depends on the polarity of the current. The latter dependence may be due to the fact that the opposite faces of the plate are not quite identical. To verify this, one face of sample Bi2, which had initially a high surface conductivity, was etched to decrease the adjacent conductivity. The measurement results for this sample are shown in Figs. 10 and 11.

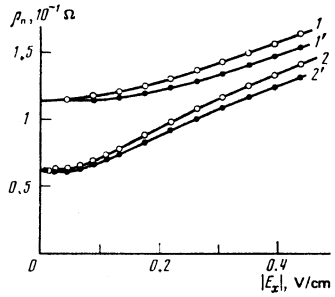

FIG. 10. Dependence of the resistivity ρ_p on the applied electric field $|E_x|$ at different polarities of E_x. Sample Bi2 was etched with HNO_3 and oxidized, after which one side was etched with $HNO_3 + H_3PO_4$. The electric current is concentrated at the one remaining oxidized side; $H = 2.89$ kOe, $T = 1.7$ K. The magnetic field is inclined to the surface; curves 1, 1') $\alpha = 8°$; 2, 2') $\alpha = 2.5°$; points • and ○ correspond to opposite polarities of E_x.

It is seen from Fig. 10 that the resistivity ρ_p does not depend on the magnitude and polarity of the electric field E_x in the plate. At a fixed field E_x, reversal of the magnetic-field direction produces the same resistivity change as reversal of the polarity of E_x:

$$\rho_p(E_x, -H) = \rho_p(-E_x, H) \neq \rho_p(E_x, H).$$

In the nonlinear region, the resistivity ρ_p can be represented as a sum of three terms, $\rho_p = R_0 + \Delta R_1 + \Delta R_2$, where R_0 is the resistance at small E_x,

$$\Delta R_1 = [\rho_p(E_x) - \rho_p(-E_x)]/2$$

is a linear resistivity increment nonlinear in E, and

$$\Delta R_2 = [\rho_p(E_x) + \rho_p(-E_x)]/2 - R_0$$

is an increment even in E_x. Figure 11 shows plots of

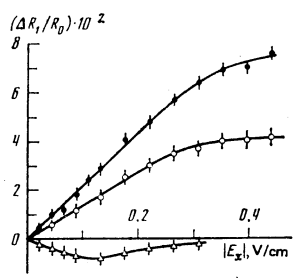

FIG. 11. Dependence of the nonlinear resistance increment odd in E_x on the electric field E_x. The points ○ were obtained by subtracting curves 1 and 1', and • by subtracting curves 2 and 2' of Fig. 10. △) points for the same sample Bi2 with faces having the same finish (oxidized under the same condition as when the light circles were obtained.

ΔR_1 vs. E_x, obtained by subtracting curve 1 from 1′ and 2 from 2′ of Fig. 10. It is seen now that the initial sections of these plots are linear, $\Delta R_1 \propto E_x$. The value of ΔR_1 in our experiments did not exceed 0.1 R_0. If the increments ΔR_1 and ΔR_2 are due to the same nonlinearity mechanism, then ΔR_2 should apparently be smaller than ΔR_1, since the expansion of ΔR_2 in powers of E_x begins with terms proportional to E_x^2 or with terms of higher even power, while $\Delta R_1 \propto E_x$. In our experiments, in electric fields $E_x \approx 0.2$–0.4 V/cm, conversely, $\Delta R_2 > \Delta R_1$ (see Fig. 10). This means that the resistance increments that are even and odd in E_x are due to different nonlinearity mechanisms.

As seen from Fig. 11, the ratio $\Delta R_1/R_0$ for the Bi2 sample with different faces is larger and of opposite sign than the sample whose faces have like finishes. This confirms the assumption that the resistance increment odd in E_x is due to the nonequivalence of the plate faces.

The nonlinear properties were investigated in a magnetic field $H \gg \rho_2/\rho_3$, where the phenomenological solution for weak electric fields and currents describes the experimental results well. We shall therefore discuss the results of the measurements of the resistance in strong electric fields within the framework of the phenomenological approach.

1. The change in sample resistance can be the result of heating of the electron system at the surface by the electric field,[13] since heating changes the times τ and T_{int}. Heating can lead to a resistance increment that is even in E_x.

2. The electric field changes the electron and hole density at the surface by an amount n'. The electron and hole Fermi levels are therefore shifted relative to each other by an amount $\Delta\mathscr{E} = n'(1/\nu_e + 1/\nu_h)$.

Since the momentum-space distance between the electron and hole valleys in bismuth is large, the phonons emitted in intervalley transitions at helium temperatures have an energy $\hbar\omega \gg kT$ (k is the Boltzmann constant). If the electrons go over from states with energy $\mathscr{E}_1$, where $\mathscr{E}_1 - \mathscr{E}_{F1} \gg kT$, into free states in another valley, with energy $\mathscr{E}_2$, where $\mathscr{E}_{F2} - \mathscr{E}_2 \gg kT$, and emit a phonon of energy $\hbar\omega = \mathscr{E}_1 - \mathscr{E}_2$, then the probability of such a process is proportional to the number of electrons of energy $\mathscr{E}_1$, multiplied by the number of free sites with energy $\mathscr{E}_2$:

$$W_{1,2} \propto \exp\left(-\frac{\mathscr{E}_1-\mathscr{E}_{F1}}{kT}\right)\exp\left(\frac{\mathscr{E}_2-\mathscr{E}_{F2}}{kT}\right) = \exp\left(-\frac{\hbar\omega-\Delta\mathscr{E}}{kT}\right).$$

If $\mathscr{E}_{F1} > \mathscr{E}_{F2}$, the probability of transitions from the first valley to the second increases with increasing $\Delta\mathscr{E}$, and the probability of transitions from the second to the first decreases. The relaxation time is

$$T_{int} \propto [\mathrm{sh}\,(\Delta\mathscr{E}/kT)/\Delta\mathscr{E}]^{-1}.$$

Since $\Delta\mathscr{E}$ increases with increasing electric field E_x, the intervalley relaxation time T_{int} decreases with increasing $|E_x|$. This leads to the *a* resistance increment ΔR_2 that is even in E_x.

The resistance-change causes 1 and 2 above explain the large resistance increments ΔR_2 that are even in E_x, but do not explain the experimentally observed odd increment ΔR_1.

3. As already noted, the Fermi energies of the carriers are changed at the surface, since the electric field changes the density of the electrons and holes. The energy change leads to changes in the Fermi velocities, the state densities, and the wavelengths of the electrons and holes, and hence also to a change in the scattering. The electron-hole recombination time T_{int} in the volume, at distances from the surface on the order of the diffusion length, and the rate S of the surface recombination, will therefore change when the electric field E_x is increased. Depending on the polarity of E_x, the Fermi velocities, the state densities, and the reciprocal wavelengths will increase or decrease; the increments of S and T_{int} will therefore be linear in E_x. At the opposite faces of the plate the increments to S and T_{int} are of opposite sign, in view of the opposite signs of n'. If, however, S is different on the different faces in weak electric fields, an odd resistance increment ΔR_1 appears, with $\Delta R_1/R_0 \sim n'/n_0$ or less.

4. The conductivity-tensor components and the values of $\beta_{e,h}$ also depend on the carrier density, so that the left-hand side of Eq. (4) is nonlinear. We have linearized this equation in order to determine the resistivity in weak electric fields. Nonlinear corrections proportional to n'/n_0 appear if S is different on opposite faces of the plate. The ratio $\Delta R_1/R_0$ can become of the order of n'/n_0.

We now compare the ratios $\Delta R_1/R_0$ and n'/n_0 in our experiments. The value of n' can be determined from Eq. (3). Integrating it over the plate thickness and discarding the small first term, we obtain $I = \sigma_H(\beta_e + \beta_h)m'$. Here I is the electric current per unit width of the plate. Account is taken of the fact that $|n'|$ is much larger at one face than at the other. Knowing I, σ_H, and $\beta_{e,h}$ we can easily determine n' and n'/n_0. In a field $E_x = 0.3$ V/cm we have $n'/n_0 \approx 0.12$. The ratio $\Delta R_1/R_0$ in the same electric field is ≈ 0.06 (see Fig. 11), meaning $\Delta R_1/R_0 \sim n'/n_0$, in accord with the mechanisms 3 and 4 above.

These mechanisms explain the resistance increments ΔR_1 that are odd in E_x, but make a small contribution to ΔR_2.

The nonlinear properties of the samples whose surface conductivity exceeds the bulk conductivity, in a field $H \gg \rho_2/\rho_3$, can be explained on the basis of the phenomenological approach. We note that the nonlinearity mechanisms in such samples are more diverse and the nonlinearity manifests itself more strongly than in samples whose bulk conductivity exceeds greatly the surface conductivity, at the same power released in the crystal.

The author is deeply grateful to V. T. Dolgopolov for constant interest in the work, helpful discussions, advice, and help, to I. N. Zhilyaev for supplying the single-crystal bismuth ingots from which some of the employed samples were cut, and to V. F. Gantmakher for discussions.

APPENDIX

1. The crystallographic axis C_3 is directed along the normal to the plate (the y axis), while the axes C_1 and C_2 are directed along x and y, respectively. The resistance is

$$\rho_p=\frac{S+p/K_1K_2T_{int}}{2(\beta_e+\beta_h)\sigma_H^2},$$

where

$$p=\frac{S_e(K_1^2+K_1K_2+K_2^2-DT_eK_1^2K_2^2)-(K_1+K_2)/T_e}{S_e(-K_1-K_2)+DK_1K_2+1/T_e},$$

$$K_{1,2}^2=\frac{AT_{int}+DT_e\pm[(AT_{int}-DT_e)^2+4BCT_{int}T_e]^{1/2}}{2(AD-BC)T_{int}T_e},\quad K_1,K_2<0,$$

$$A=\frac{\sigma_e\sigma_h(\beta_e+\beta_h)}{(\sigma_e+\sigma_h)e},\quad B=\frac{2\beta_e\sigma_h(\sigma_{e_1}-\sigma_{e_2})}{(\sigma_e+\sigma_h)e},$$

$$C=\frac{\sigma_h(\sigma_{e_1}-\sigma_{e_2})(\beta_e+\beta_h)}{(\sigma_e+\sigma_h)e},\quad D=\frac{\beta_e(9\sigma_{e_1}\sigma_{e_2}+2\sigma_{e_1}\sigma_h+\sigma_{e_2}\sigma_h)}{(\sigma_e+\sigma_h)e}$$

Here σ_{e1}, σ_{e2}, and σ_h are the σ_{yy} components of the conductivity tensors of the electron and hole valleys. For two of the three electron valleys these components are equal to each other. The conductivities are

$$\sigma_i=\sigma_{yy}'=\sigma_2^i+\alpha^2\sigma_3^i,$$

where $i=e_1$, e_2, and h. The quantities $i/3$ do not depend on the magnetic field, $\sigma_2^i\sim\sigma_3^i(r/l)^2$. σ_H and β_e contain the combined electron density and the electron-state density. We have next

$$S_e=Sv_h/(v_e+v_h)+3S_{ee},$$

where S_{ee} is the rate of the surface relaxation between two electron valleys

$$1/T_e=v_h/(v_e+v_h)T_{int}+3/T_{ee},$$

where T_{ee} is the relaxation time between two electron valleys in the interior of the sample.

At $(r/l)^2\ll\alpha^2\ll1$ the values of K_1 and K_2 do not depend on the magnetic field, and $|K_1|$, $|K_2|\sim1/|\alpha|$. We introduce K_1' and K_2' such that $K_1=K_1'/|\alpha|$ and $K_2=K_2'/|\alpha|$; then

$$\frac{p}{K_1K_2}=|\alpha|\frac{1}{K_1'K_2'}\left\{S_e[(K_1')^2+K_1'K_2'+(K_2')^2-DT_e(K_1')^2(K_2')^2]-\frac{K_1'+K_2'}{T_e}|\alpha|\right\}[S_e(-K_1'-K_2')+(DK_1'K_2'+1/T_e)|\alpha|]^{-1}.$$

In a number of limiting cases, when $p/K_1K_2\sim\alpha$, the resistivity can be represented in the form $\rho_p=\rho_0+|\alpha|\rho_1$ where, as in the case of the two-valley model, $\rho_0\propto H^2$ and $\rho_1\propto H^2$.

2. The crystallographic axis C_3 is directed along the z axis, and C_1 and C_2 are directed along x or y each. In this case $\sigma_3^{e1}=\sigma_3^{e2}=\sigma_3^{e3}$. At $(r/l)^2\ll\alpha^2\ll1$ we have

$$K_1=-\frac{1}{(AT_{int})^{1/2}}=-\frac{1}{L_{int}},\quad K_2=-\frac{1}{(DT_e)^{1/2}}=-\frac{1}{L_e}.$$

The boundary conditions are more complicated than in the preceding case, since the electrons from the different valleys are differently scattered by the surface. The resistance is

$$\rho_p=\left(S-\frac{\Delta S^2}{S_e+L_e/T_e}+\frac{L_{int}}{T_{int}}\right)e\Big/2(\beta_e+\beta_h)\sigma_H^2;$$

here

$$S=1/3(S_{e_1h}+2S_{e_2h})(1+\nu_e/\nu_h),\quad S_e=1/3(2S_{e_1h}+S_{e_2h})+3S_{e_1e_2},$$
$$\Delta S=(S_{e_1h}-S_{e_2h})[2/9(1+\nu_e/\nu_h)]^{1/2}.$$

The constants $S_{e_1e_2}$, S_{e_1h}, S_{e_2h} describe the intervalley scattering of the carriers by the surface, ν_e is the combined state density of the electrons. If $S_e\gg L_e/T_e$ or $S_e\ll L_e/T_e$, then ρ_p can be represented in the form $\rho_p=\rho_0+|\alpha|\rho_1$, where ρ_0 and $\rho_1\propto H^2$, and ρ_1 satisfies Eq. (11) in which $\sigma_3=\sigma_3^{e1}+\sigma_3^{e2}+\sigma_3^{e3}$.

[1]M. Ya. Azbel', Zh. Eksp. Teor. Fiz. **44**, 983 (1963) [Sov. Phys. JETP **17**, 667 (1963)].
[2]M. Ya. Azbel' and V. G. Peschanskiĭ, *ibid.* **49**, 572 (1965) [**22**, 399 (1966)].
[3]V. G. Peschanskiĭ and M. Ya. Azbel', *ibid.* **55**, 1980 (1968) [**28**, 1045 (1969)].
[4]A. I. Kopeliovich, *ibid.* **78**, 987 (1980) [**51**, 498 (1980)].
[5]T. Hattori, J. Phys. Soc. Jpn. **23**, 19 (1967).
[6]G. I. Babkin and V. Ya. Kravchenko, Zh. Eksp. Teor. Fiz. **60**, 695 (1971) [Sov. Phys. JETP **33**, 378 (1971)].
[7]Yu. A. Bogod, V. V. Eremenko, and L. K. Chubova, *ibid.* **56**, 32 (1969) [**29**, 17 (1969)].
[8]Yu. A. Bogod and Vit. B. Krasovitskiĭ, Fiz. Kondens. sost., No. 30, Khar'kov, 1974, p. 11.
[9]É. I. Rashba, Z. S. Gribnikov, and V. Ya. Kravchenko, Usp. Fiz. Nauk **119**, 3 (1976) [Sov. Phys. Usp. **19**, 361 (1976)].
[10]A. A. Lopez, Phys. Rev. **175**, 823 (1968).
[11]H. K. Collan, M. Krusins, and G. R. Pickett, Phys. Rev. **B1**, 2888 (1970).
[12]Krishna Man Mohan and B. N. Sirvastava, Sol. St. Comm. **12**, 433 (1973).
[13]S. S. Murzin and V. T. Dolgopolov, Zh. Eksp. Teor. Fiz. **79**, 2282 (1980) [Sov. Phys. JETP **52**, 1155 (1980)].

Translated by J. G. Adashko